

GDF10 blocks hepatic PPAR γ activation to protect against diet-induced liver injury



Khrystyna Platko^{1,4}, Paul F. Lebeau^{1,4}, Jae Hyun Byun¹, Samantha V. Poon¹, Emily A. Day², Melissa E. MacDonald¹, Nicholas Holzapfel¹, Aurora Mejia-Benitez¹, Kenneth N. Maclean³, Joan C. Krepinsky¹, Richard C. Austin^{1,*}

ABSTRACT

Objective: Growth differentiation factors (GDFs) and bone-morphogenic proteins (BMPs) are members of the transforming growth factor β (TGF β) superfamily and are known to play a central role in the growth and differentiation of developing tissues. Accumulating evidence, however, demonstrates that many of these factors, such as BMP-2 and -4, as well as GDF15, also regulate lipid metabolism. GDF10 is a divergent member of the TGF β superfamily with a unique structure and is abundantly expressed in brain and adipose tissue; it is also secreted by the latter into the circulation. Although previous studies have demonstrated that overexpression of GDF10 reduces adiposity in mice, the role of circulating GDF10 on other tissues known to regulate lipid, like the liver, has not yet been examined.

Methods: Accordingly, GDF10^{-/-} mice and age-matched GDF10^{+/+} control mice were fed either normal control diet (NCD) or high-fat diet (HFD) for 12 weeks and examined for changes in liver lipid homeostasis. Additional studies were also carried out in primary and immortalized human hepatocytes treated with recombinant human (rh)GDF10.

Results: Here, we show that circulating GDF10 levels are increased in conditions of diet-induced hepatic steatosis and, in turn, that secreted GDF10 can prevent excessive lipid accumulation in hepatocytes. We also report that GDF10^{-/-} mice develop an obese phenotype as well as increased liver triglyceride accumulation when fed a NCD. Furthermore, HFD-fed GDF10^{-/-} mice develop increased steatosis, endoplasmic reticulum (ER) stress, fibrosis, and injury of the liver compared to HFD-fed GDF10^{+/+} mice. To explain these observations, studies in cultured hepatocytes led to the observation that GDF10 attenuates nuclear peroxisome proliferator-activated receptor γ (PPAR γ) activity; a transcription factor known to induce *de novo* lipogenesis.

Conclusion: Our work delineates a hepatoprotective role of GDF10 as an adipokine capable of regulating hepatic lipid levels by blocking *de novo* lipogenesis to protect against ER stress and liver injury.

© 2019 The Authors. Published by Elsevier GmbH. This is an open access article under the CC BY-NC-ND license (<http://creativecommons.org/licenses/by-nc-nd/4.0/>).

Keywords BMP-3b; ER stress; Hepatic steatosis; HFD; NAFLD; NASH; TGF β

1. INTRODUCTION

Obesity is considered by many as the epidemic of the 21st century, affecting over 2 billion individuals worldwide and still increasing in frequency [1]. Although obesity is commonly thought of as a disease characterized by excess adipose tissue, other hallmark characteristics are also common in obese individuals. Non-alcoholic fatty liver disease (NAFLD) affects approximately 75% of obese individuals and contributes to other comorbidities associated with obesity, such as type 2 diabetes mellitus, hypertension, heart disease and ischemic stroke [2,3]. NAFLD is defined as an accumulation of triglyceride in the liver in excess of 5% of total liver weight and is commonly referred to as steatosis. Simple steatosis is largely benign; however, NAFLD can progress to life-threatening non-alcoholic steatohepatitis (NASH) or liver cirrhosis. Although the precise mechanism of progression remains

poorly understood, the well-accepted *multiple-hits hypothesis* suggests that cellular events including oxidative stress, lipid peroxidation, Kupffer cell activation, and adipocytokine alterations play a central role [1,4]. Numerous studies have also demonstrated that ER stress plays a key role in the development of NAFLD and NASH by promoting Kupffer cell activation, oxidative stress and mitochondrial dysfunction [5–7]. Given that secretory cells like adipocytes and hepatocytes are rich in ER, the role of ER stress has become a topic of considerable interest in the development of metabolic diseases. ER stress is characterized by an overwhelming of ER-resident chaperones by misfolded *de novo* polypeptides in the ER lumen. This event triggers the unfolded protein response (UPR) in order to increase ER protein folding capacity and restore homeostatic conditions. The signaling cascades of the UPR are comprised of (a) the activating transcription factor 6 (ATF6) pathway, which modulates sterol regulatory element-binding protein (SREBP)-2

¹Department of Medicine, McMaster University, The Research Institute of St. Joe's Hamilton, Hamilton Centre for Kidney Research, Hamilton, Ontario, L8N 4A6, Canada ²The Division of Endocrinology and Metabolism, Department of Medicine, McMaster University, 1280 Main Street West, Hamilton, Ontario, L8N 4A6, Canada ³The Department of Pediatrics, University of Colorado School of Medicine, Aurora, CO, 80045, USA

⁴ Khrystyna Platko and Paul F. Lebeau contributed equally to this work.

*Corresponding author. 50 Charlton Ave East, Room T-3313, Hamilton, Ontario, L8N 4A6, Canada. Fax: +905 540 6589. E-mail: austinr@taari.ca (R.C. Austin).

Received April 9, 2019 • Revision received June 14, 2019 • Accepted June 24, 2019 • Available online 28 June 2019

<https://doi.org/10.1016/j.molmet.2019.06.021>

Abbreviations

ANGPTL4	angiopoietin-like 4	IHC	immunohistochemistry
ACOX1	acyl-coenzyme A oxidase 1	IAT	inguinal adipose tissue
ACOT2	acyl-coenzyme A thioesterase 2	IRE1 α	inositol-requiring 1 α
ACADM	acyl-coenzyme A dehydrogenase, C-4 to C-12 straight chain	LPL	lipoprotein lipase
ATF4	activating transcription factor 4	IL1 β	interleukin 1 β
ATF6	activating transcription factor 6	LDH	lactate dehydrogenase
ALT	alanine-L transaminase	NAFLD	non-alcoholic fatty liver disease
BMP	bone morphogenic protein	NASH	non-alcoholic steatohepatitis
BAT	brown adipose tissue	NCD	normal control diet
BSA	bovine-serum albumin	ORO	Oil Red O
C/EBP α	CCAAT-enhancer-binding protein α	OA	oleate
CD36	cluster of differentiation 36	PFA	paraformaldehyde
CGTZ	ciglitizone	PPAR γ/α	peroxisome proliferator-activated receptor γ/α
CLAMS	Columbus Instruments Comprehensive Lab Animal Monitoring System	PGC1 β	peroxisome proliferator-activated receptor gamma coactivator 1- β
CRTC2	CREB-regulated transcription cofactor 2	PPRE	peroxisome proliferator response element
CHOP	C/EBP homologous protein	PSR	Picrosirius red
DMEM	Dulbecco's Modified Eagle's Medium	PDK4	pyruvate dehydrogenase lipoamide kinase isozyme 4
ER	endoplasmic reticulum	PERK	protein kinase RNA (PKR)-like ER kinase
FBS	fetal bovine serum	PA	palmitate
FATP5	fatty acid transport protein 5	PCK1	phosphoenolpyruvate carboxykinase 1
FSP27	fat-specific protein 27	PBS	phosphate-buffered saline
FOXO1	forkhead box protein O1	rhGDF10	recombinant human growth differentiation factor 10
FN1	fibronectin 1	si	small interfering
FFPE	formalin-fixed paraffin-embedded	STAT3	signal transducer and activator of transcription 3
GDF10	growth differentiation factor 10	SREBP-1/-2	sterol regulatory element-binding protein-1/-2
GAT	gonadal adipose tissue	TGF β	transforming growth factor β
GRP78	glucose-regulated protein of 78 kDa	TGF β R1	TGF β receptor subtype-1
GRP94	glucose-regulated protein of 94 kDa	TG	thapsigargin
β -HB	β -hydroxybutyrate	TM	tunicamycin
HFD	high-fat diet	TNF α	tumor necrosis factor alpha
		UPR	unfolded protein response
		XBP1	X-box-binding protein 1

mediated *de novo* lipogenesis [8]; (b) the highly conserved inositol-requiring 1 α (IRE1 α) - X-box-binding protein 1 (XBP1) pathway, which is required for the regulation of hepatic lipids during conditions of stress [9]; as well as (c) the protein kinase RNA (PKR)-like ER kinase (PERK) - activating transcription factor 4 (ATF4) pathway capable of regulating *de novo* lipogenesis via fatty acid synthase and SREBP-1 [10]. Previous studies have also demonstrated that ATF4 can induce the expression and activation of PPAR γ , a transcription factor known to promote the expression of pro-adipogenic mediators including fatty acid transport protein 5 (*FATP5*), angiopoietin-like 4 (*ANGPTL4*), lipoprotein lipase (*LPL*), *Perilipin*, cluster of differentiation 36 (*CD36*) and fat-specific protein 27 (*FSP27*) [11,12]. Clinical studies have also characterized increased PPAR γ expression in the livers of patients with NAFLD [13]. Although pro-survival at its core, chronic or severe ER stress can induce the expression of lipid-regulatory genes that promote *de novo* lipogenesis, as well as drive inflammation, fibrosis, and apoptosis in the liver [14].

GDF10, also known as BMP-3b, is an atypical member of the TGF β superfamily capable of inhibiting osteoblast differentiation by antagonizing BMP-2 and -4 mediated osteogenesis [15]. To date, over 30 members of the superfamily have been described, and all share common features. They are synthesized as precursor proteins containing N-terminal signal peptide sequences and pro-regions. Once secreted, the mature, biologically active molecule is believed to consist

of a homodimer originating from proteolytically-cleaved precursors [16]. In recent years, accumulating evidence has shown that these factors play a central role in the regulation of energy balance and homeostasis. BMP-2 and -4 promote white adipogenesis while BMP-7 promotes brown adipogenesis [17–19]. Studies have also demonstrated that *in vitro* knockdown of GDF10 enhances adipogenesis and that transgenic mice overexpressing GDF10 are protected against diet-induced obesity and insulin resistance [20,21]. GDF15 has also been shown to regulate feeding and fatty acid oxidation and to protect against steatosis, insulin resistance, obesity, and ER stress in the livers of mice fed a HFD [22–24].

It is well-established that adipokines can modulate obesity and a variety of its comorbidities, including NAFLD [25]. However, little is known about the role of circulating GDF10 on liver health/function and injury in the face of diet-induced obesity. Here, we report that pharmacologic and diet-induced ER stress increases the expression of GDF10 in cultured pre-adipocytes and in white adipose tissue. We also show that GDF10^{-/-} mice exhibit increased nuclear PPAR γ expression and activity coupled with hepatic steatosis on the NCD and develop a severe NASH-like phenotype on the HFD. Collectively, our findings suggest that circulating GDF10 plays a critical role as a regulator of hepatic PPAR γ during conditions of dietary stress and that GDF10 is capable of attenuating the progression of steatosis to NASH.

2. MATERIALS AND METHODS

2.1. Animal studies

GDF10^{-/-} mice were a generous gift from Dr. Se-Jin Lee (Johns Hopkins University) [16]. Animals were housed in 12 h light cycles and controlled temperature and humidity conditions and had access to standard NCD (2918, Envigo) and water *ad libitum* (n = 10). In experiments designed to study diet-induced hepatic steatosis, male GDF10^{-/-} mice and age-matched GDF10^{+/+} controls were provided with HFD (60% Kcal; TD.06414, Envigo) *ad libitum* starting at 6 weeks of age for an additional 12 weeks prior to sacrifice (n = 5). Measurements of metabolic parameters were performed using the Columbus Instruments Comprehensive Lab Animal Monitoring System (CLAMS) one week prior to sacrifice. A cohort of 12-week-old male C57BL/6J mice were also treated with phosphate-buffered saline (PBS) vehicle control or with the ER stress-inducing agent, tunicamycin (TM; 500 µg/kg), for 24 h via intraperitoneal injection in the left flank (n = 5). All mice were fasted for 6 h and anesthetized using isoflurane prior to sacrifice. Experimental procedures were approved by the McMaster University Animal Research Ethics Board.

2.2. Cell culture and treatment

Huh7 and HepG2 immortalized human hepatocyte cell lines as well as primary human hepatocytes were maintained in 5% CO₂ at 37 °C and cultured in Dulbecco's Modified Eagle's Medium (DMEM) or Willams' E medium, supplemented with 10% v/v fetal bovine serum (FBS), 100 IU/ml penicillin and 100 µg/ml streptomycin. For experimental procedures designed to examine the effect of GDF10 on lipid accumulation, cells were pre-treated with rhGDF10 (250 ng/mL, R&D Systems) for 24 h and then treated with agents known to stimulate lipid droplet accumulation, such as oleate (OA; 200 µM, Sigma—Aldrich), palmitate (PA; 200 µM, Sigma—Aldrich), thapsigargin (TG; 100 nM, Sigma—Aldrich) and TM (2 µg/mL, Sigma—Aldrich) for an additional 24 h. Similarly, for studies examining the effect of GDF10 on PPAR γ -mediated lipid accumulation, hepatocytes were pre-treated with rhGDF10 and then treated with PPAR γ agonist, ciglitzone (CGTZ; 10 µM, Tocris Bioscience), for 24 h prior to analysis. For experiments designed to examine the effect of GDF10 on PPAR γ cellular localization and promoter binding, cells were pre-treated with rhGDF10 for 24 h, and subsequently treated with CGTZ for 1 h prior to analysis. All cell culture experiments were repeated a minimum of 3 times. To block Smad3 expression, siGENOME SMARTpool siRNA targeted against Smad3 (UCAAGAGCCUGGUCAAGAA, GAGUUCGCCUCAAUAUGA, GGACGAGGUUCUC-CAAAC, GGACGAGGUCUGCGUAAU) was purchased from Dharmacon (SO-2782081G). 100 nM of siRNA targeted against Smad3 or scrambled siRNA control was transfected using RNAiMAX (ThermoFisher Scientific) as described previously [26].

2.3. Cell fractionation and transcriptional activity studies

Huh7 and HepG2 cells were seeded into 100 mm dishes and allowed to grow to confluency of 80%. Following treatment, nuclear and cytosolic fractions were isolated using an extraction kit (Abcam) according to the manufacturer's instructions. For experiments designed to examine the effect of GDF10 on PPAR γ transcriptional activity, HepG2 cells were pre-treated with rhGDF10 for 24 h, and subsequently treated with CGTZ for 1 h prior to cellular fractionation. PPAR γ transcription factor assay kit (Abcam) was carried out according to manufacturer's instructions. Briefly, 120 µg of protein isolated from nuclear extracts was added to each well of a 96-well plate coated with a double-stranded DNA sequence containing peroxisome proliferator response element (PPRE). Following an over-night incubation, anti-

PPAR γ primary antibody was added, followed by an HRP-conjugated secondary antibody. PPAR γ binding to the PPRE was detected using a spectrophotometer at a wavelength of 450 nm.

2.4. Histological and immunohistochemical staining

Histological analysis was carried out in formalin-fixed paraffin-embedded (FFPE) tissues that were cut into 4 µm thick sections. Gross pathological changes were first examined with hematoxylin and eosin (H&E) and collagen accumulation was examined using Mason's Trichrome (Sigma—Aldrich). Analysis of intracellular triglyceride accumulation was carried out in OCT-embedded liver sections (10 µm) and in cultured cells fixed in 4% paraformaldehyde (PFA) using Oil Red O (ORO). The ORO content of isopropanol extracts was measured using a spectrophotometer (Molecular Devices) at a wavelength of 520 nm [27]. Immunohistochemical (IHC) staining was also carried out in 4 µm thick FFPE sections. Briefly, deparaffinized sections were blocked in 5% serum, incubated in primary antibody for 18 h at 4 °C, and exposed to biotin-labeled secondary antibody (Vector Laboratories; for a complete list of antibodies and working dilutions, please refer to Supplemental Table 1). Streptavidin-labeled HRP solution (Vector Laboratories) and the developing solution (Vector Laboratories) were used to visualize staining. Slides were examined using a Nikon microscope and images were quantified using ImageJ Software (NIH).

2.5. Quantitative real time PCR

Total RNA was isolated using RNA purification kits (ThermoFisher Scientific). A total of 2 µg of RNA was reverse transcribed to cDNA using the High-Capacity cDNA Reverse Transcription Kit (Applied Biosystems). PCR amplification was performed using the Fast SYBRGreen PCR master mix (Applied Biosystems) according to the manufacturer's instructions. All primer sequences are listed in Supplemental Table 2.

2.6. Immunoblots

Whole cell and tissue lysates were prepared using SDS lysis buffer containing a protease inhibitor cocktail (Roche), and protein concentration was measured as described previously [26]. The samples were resolved using SDS-PAGE and subsequently transferred to nitrocellulose membranes. Nitrocellulose membranes were then incubated in 5% w/v skimmed milk and primary antibody followed by the respective secondary antibody. The signal was detected using a Konica Minolta X-Ray film processor.

2.7. Immunofluorescent staining

Following treatment, Huh7 and primary human hepatocytes were fixed in 4% PFA and permeabilized in 0.025% Triton X-100 for 15 min. After blocking in 5% bovine-serum albumin (BSA), cells were stained with primary antibody, washed, and subsequently stained with fluorescently-labeled secondary antibodies and DAPI nuclear stain. Slides were then mounted using an aqueous mounting medium (ThermoFisher Scientific) and visualized using the EVOS FL (ThermoFisher Scientific) imaging system.

2.8. Plasma β -hydroxybutyrate (β -HB), ELISA, lactate dehydrogenase (LDH) and alanine-L transaminase (ALT) assays

Plasma levels of the ketone body β -HB were measured using a colorimetric assay (Cayman). Circulating GDF10 levels were measured using a mouse GDF10 ELISA kit (Elabscience). Plasma ALT was measured using a commercially available colorimetric assay (Abcam). Cytotoxicity was examined using a LDH colorimetric assay kit (Roche). All assays were performed according to the manufacturer's instructions.

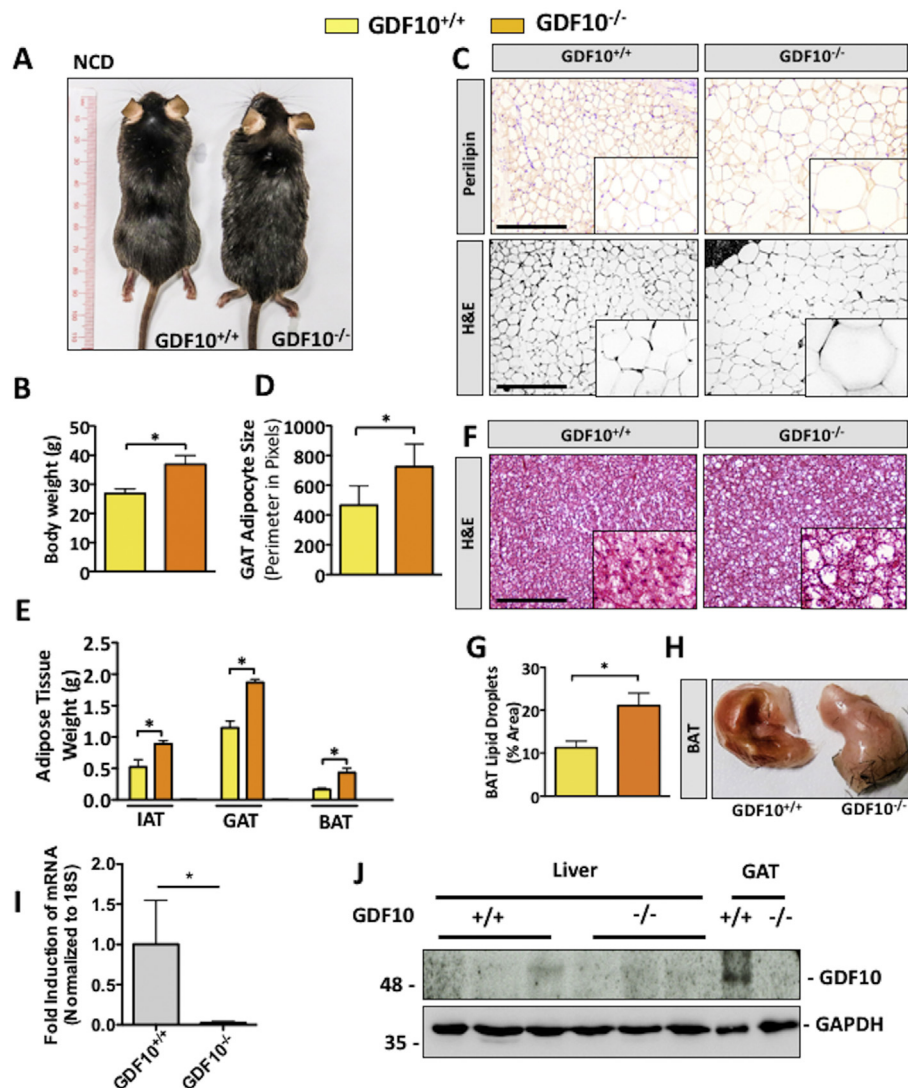


Figure 1: GDF10^{-/-} mice have increased body weight and adiposity. (A) Macroscopic appearance and (B) body weights of 30 week old GDF10^{+/+} and GDF10^{-/-} mice fed NCD (n = 5). (C) IHC staining of the adipocyte marker perlipin and H&E staining of the GAT. (D) Average adipocyte size in GAT. (E) Weights of the IAT, GAT, and BAT. (F) H&E staining of the BAT. (G) Quantification of lipid droplets in BAT using ImageJ software. (H) Macroscopic appearance of the BAT from GDF10^{+/+} and GDF10^{-/-} mice at 30 weeks of age. (I) Real time PCR analysis of mRNA abundance of GDF10 in the GAT to confirm knockout (n = 5). (J) Immunoblots of the liver and GAT from GDF10^{+/+} and GDF10^{-/-} mice. Scale bars, 100 μ m. All data are shown as the mean \pm S.D. *, $p < 0.05$ by unpaired two-tailed Student's t -test.

2.9. Quantification of plasma, hepatic, and fecal lipid

Equal amounts of liver tissues were lysed in a mixture of hexane/2-propanol and incubated on an orbital shaker at 37 °C for 5 h. Samples were then subjected to centrifugation for 5 min (12,000 rpm) in order to isolate the lipid-containing liquid phase. Lipid content was quantified using a colorimetric triglyceride assay (Wako Diagnostics) according to the manufacturer's instructions. In a similar manner, fecal cholesterol content was measured directly from feces normalized to dry weight. Hepatic cholesterol content was measured using a commercially available colorimetric kit (Abcam) according to the manufacturer's instructions.

2.10. Statistical analysis

Data are reported as the mean \pm SD. Statistical analysis was performed using GraphPad Prism. For comparison between two groups, an unpaired two-tailed Student's t -test was used. For analysis of three or more groups, a one-way ANOVA followed by Tukey's HSD multiple

comparison test was performed. Differences between groups were considered statistically significant when $p < 0.05$.

3. RESULTS

3.1. GDF10^{-/-} mice exhibit increased body weight gain and adiposity

Increased body weight gain in our GDF10^{-/-} mouse colony was among our initial observations and was consistently observed in mice fed NCD (Figure 1A,B; *, $p < 0.05$, n = 5). Following this observation, adiposity was examined via IHC staining for the adipocyte marker, perlipin, as well as H&E of the gonadal adipose tissue (GAT). Consistent with gross morphological observations, GDF10^{-/-} mice had increased mean adipocyte size (Figure 1C,D; *, $p < 0.05$, n = 5) and weight of the inguinal adipose tissue (IAT), GAT and brown adipose tissue (BAT) (Figure 1E; *, $p < 0.05$, n = 5). BAT from GDF10^{-/-} mice also appeared lighter in color and revealed increased lipid droplets

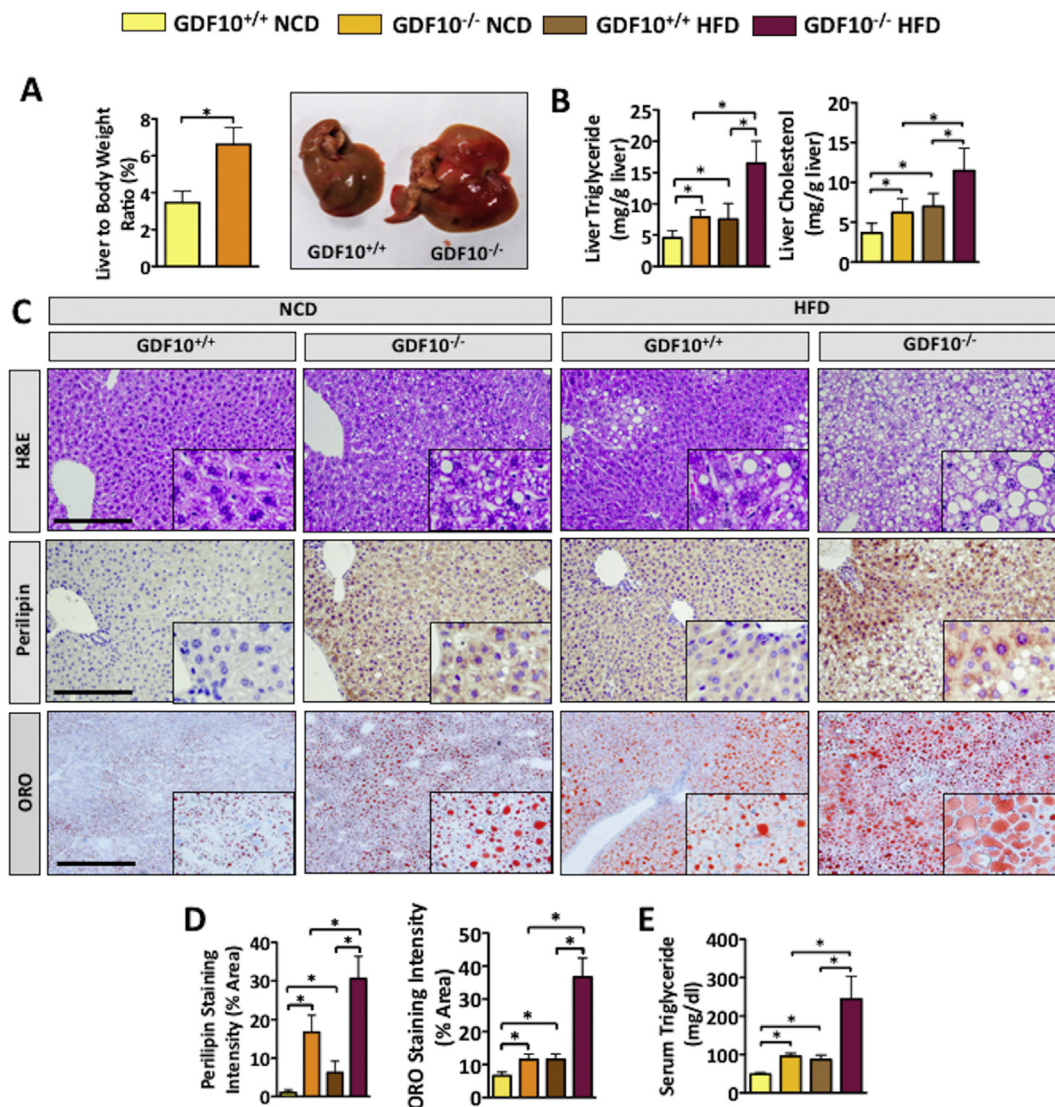


Figure 2: GDF10 deficiency leads to hepatic lipid accumulation. (A) Weights and macroscopic appearance of the livers from NCD-fed GDF10^{+/+} and GDF10^{-/-} mice (n = 5). (B) Hepatic triglyceride and cholesterol content (n = 5). (C) H&E, perilipin and ORO staining of livers from GDF10^{+/+} and GDF10^{-/-} mice fed NCD or HFD. (D) Quantification of perilipin and ORO staining using ImageJ Software (n = 5). (E) Serum triglyceride content. Scale bar, 100 μ m. All data are shown as the mean \pm S.D. *, $p < 0.05$ by unpaired two-tailed Student's *t*-test or one-way ANOVA.

compared to BAT from control mice (Figure 1F,G and H; *, $p < 0.05$, n = 5). GDF10 knockout was confirmed in these mice via real time PCR in GAT (Figure 1I; *, $p < 0.05$) and immunoblot (Figure 1J). Immunoblot analysis also revealed that GDF10 is expressed in GAT, but not in the livers of healthy wild-type mice (Figure 1J).

3.2. GDF10^{-/-} mice exhibit hepatic lipid accumulation

Given that steatosis is commonly observed in obese patients as well as in rodent models of obesity [1,4], we next examined the livers of GDF10^{-/-} mice fed NCD and HFD. Consistent with our observations in adipose tissue, liver weight was increased in GDF10^{-/-} mice compared to controls on the NCD (Figure 2A; *, $p < 0.05$, n = 5). Analysis of hepatic triglyceride and cholesterol content yielded findings that were consistent with liver weights (Figure 2B; *, $p < 0.05$, n = 5). Similarly, H&E, perilipin and ORO staining also revealed increased lipid

accumulation in the livers of NCD- and HFD-fed GDF10^{-/-} mice compared to wild-type counterparts (Figure 2C). To confirm our visual observations, perilipin and ORO staining was quantified using ImageJ software (Figure 2D; *, $p < 0.05$, n = 5). In line with increased hepatic lipid accumulation, an increase in plasma triglyceride content was also observed in GDF10^{-/-} compared to GDF10^{+/+} mice (Figure 2E; *, $p < 0.05$). The ability of GDF10 to modulate lipid droplet accumulation was then examined in immortalized human HepG2 cells. Consistent with *in vivo* findings, exogenously added rhGDF10 markedly reduced lipid accumulation in hepatocytes, resulting from exposure to the fatty acid, PA, and to the ER stress-inducing agent, TG (Fig. S1A; *, $p < 0.05$). Exogenously added rhGDF10 also reduced cytotoxicity resulting from the treatment of cells with ER stress-inducing agents known to cause *de novo* lipogenesis [28], TG and TM (Fig. S1B; *, $p < 0.05$).

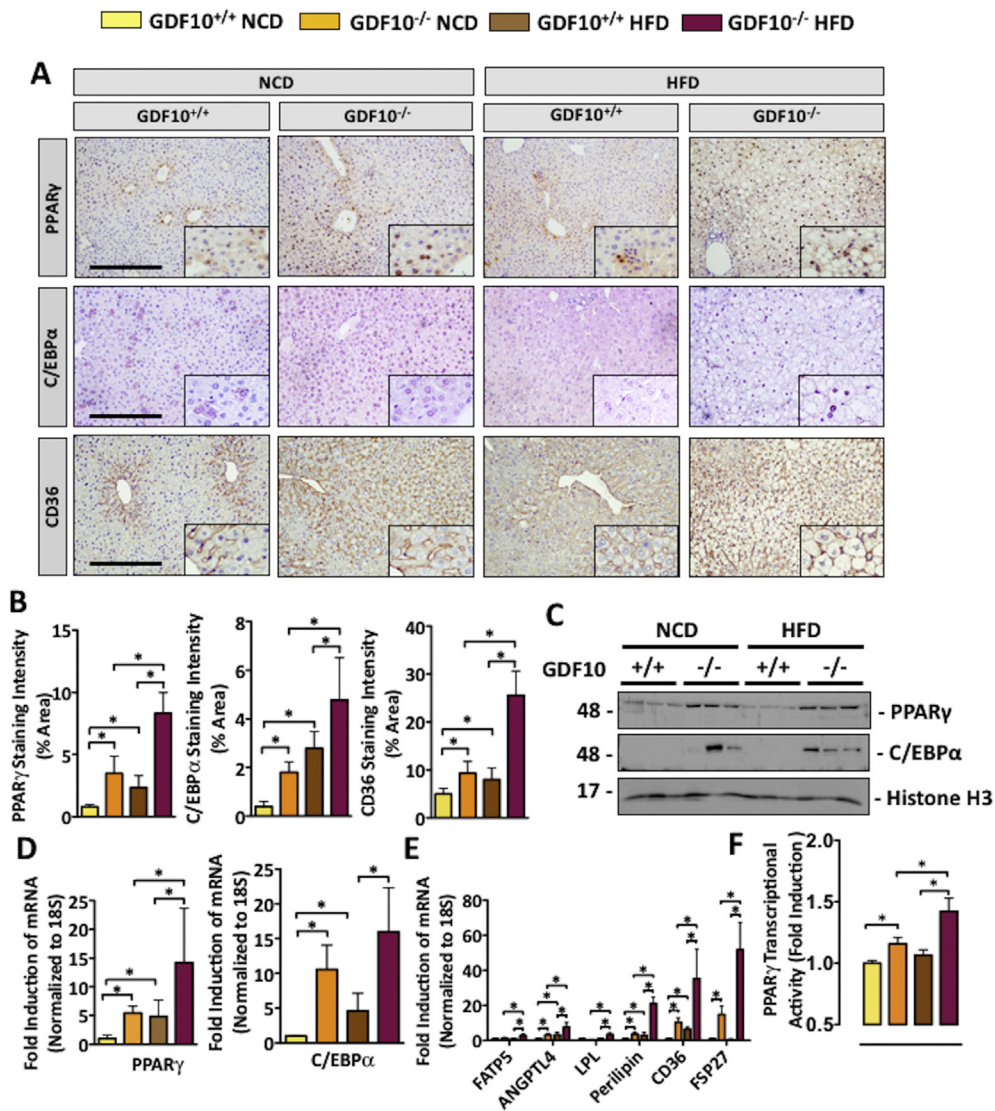


Figure 3: GDF10 deficiency increases the nuclear abundance of hepatic PPAR γ and C/EBP α . (A) IHC staining of PPAR γ , C/EBP α and CD36 in the livers of mice fed NCD or HFD. (B) Quantification of indicated histological staining. (C) Immunoblots of the nuclear subcellular fraction from livers of the mice fed NCD or HFD. (D) Real time PCR analysis of hepatic mRNA abundance of PPAR γ , C/EBP α and (E) mRNA abundance of PPAR γ -regulated genes. (F) PPAR γ transcription factor activity assay. Scale bar, 100 μ m. All data are shown as the mean \pm S.D. *, $p < 0.05$ by one-way ANOVA.

3.3. GDF10 reduces PPAR γ expression via the TGF β R1-Smad3 pathway in hepatocytes

Given the abundance of triglyceride observed in the livers of GDF10^{-/-} mice, we next assessed the expression of established modulators of *de novo* lipogenesis and lipid uptake.

Previous studies have demonstrated that mouse models of steatosis exhibit increased PPAR γ expression and activity [29]; thus, it was among the first markers examined. It is also well-known that naturally occurring derivatives of long-chain polyunsaturated fatty acids, including palmitic, linoleic, linolenic, and arachidonic acids, can activate PPAR receptor transcriptional activity [30,31]. Upon assessment of these mice, IHC staining revealed an increase in PPAR γ expression in the livers of NCD- and HFD-fed GDF10^{-/-} mice compared to controls. The expression of pro-adipogenic PPAR γ -responsive proteins, including C/EBP α and CD36, were also increased (Figure 3A,B; *, $p < 0.05$, $n = 5$). Immunoblot analysis of nuclear fractions from the livers of NCD- and HFD-fed mice revealed consistent findings, whereby

an increase in PPAR γ and C/EBP α was observed in GDF10^{-/-} compared to GDF10^{+/+} mice (Figure 3C; $n = 3$). The mRNA transcript abundance of PPAR γ and C/EBP α was also increased in the livers of NCD- and HFD-fed GDF10^{-/-} (Figure 3D; *, $p < 0.05$, $n = 5$), as was the expression of CD36 and other PPAR γ -responsive targets including FATP5, ANGPTL4, LPL, Perilipin and FSP27 (Figure 3E; *, $p < 0.05$, $n = 5$). Further examination of PPAR γ using an ELISA-based transcription factor assay [32,33] revealed a concomitant increase in the binding of PPAR γ to its PPPE, indicative of increased transcriptional activity in the livers of GDF10^{-/-} mice compared to controls (Figure 3F; *, $p < 0.05$, $n = 5$). Given its established role in the regulation of feeding and metabolism, circulating leptin was also examined in a cohort of 30 week old NCD-fed GDF10^{-/-} mice and age-matched controls. Consistent with previous reports in which PPAR γ activation was inversely correlated with leptin, we observed leptin levels to be approximately 2-fold lower in GDF10^{-/-} mice (Fig. S2; *, $p < 0.05$; $n = 7$) [34].

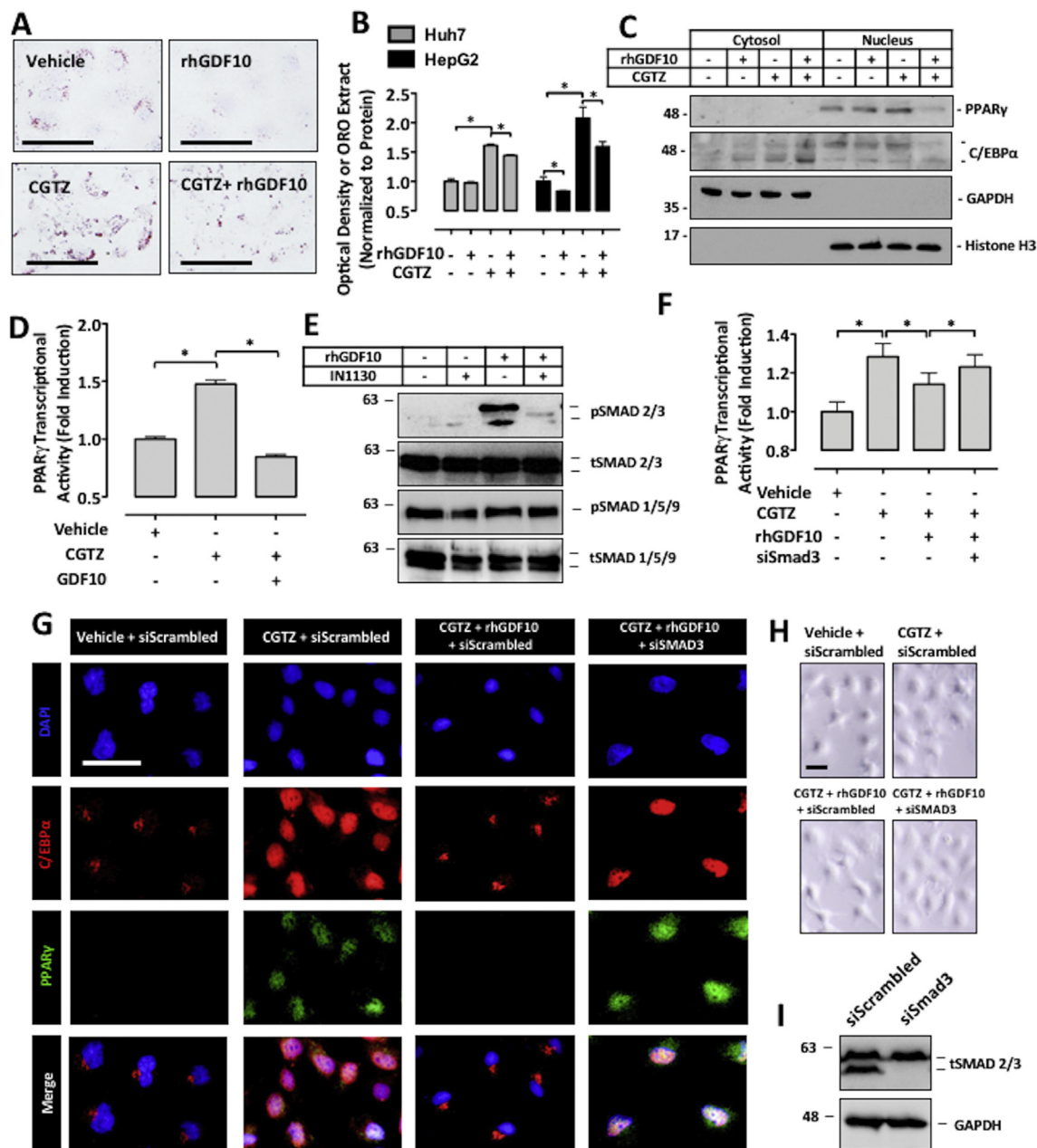


Figure 4: GDF10 modulates PPAR γ nuclear abundance and transcriptional activity. (A) ORO staining and (B) extract quantification of HepG2 cells treated with PPAR γ agonist, CGTZ (10 μ M), or rhGDF10 (250 ng/mL) for 24 h. (C) Immunoblots of the nuclear and cytosolic subcellular fractions of Huh7 cells treated with CGTZ or rhGDF10. (D) PPAR γ transcription factor activity assay after treatment with rhGDF10 or CGTZ for 1 h. (E) Immunoblots of HepG2 cells treated with IN1130 (100 nM) or rhGDF10. (F) PPAR γ transcription factor activity assay in HepG2 cells transfected with either siRNA targeted against Smad3 or scrambled control siRNA and subsequently treated with CGTZ or rhGDF10. (G) Immunofluorescent staining of PPAR γ and C/EBP α in Huh7 cells transfected with siRNA targeted against Smad3 and treated with rhGDF10 or CGTZ. (H) Morphology of the Huh7 cells was examined using a light microscope. (I) Immunoblots of HepG2 cells transfected with either siRNA targeted against Smad3 or scrambled control siRNA to confirm knock-down. Scale bars, 50 μ m. All data are shown as the mean \pm S.D. *, $p < 0.05$ by one-way ANOVA.

To substantiate our findings on the inhibitory effect of GDF10 on PPAR γ -mediated lipid droplet accumulation, cultured HepG2 and Huh7 immortalized human hepatocytes were pre-treated with rhGDF10 and exposed to CGTZ, an established glitazone agonist of PPAR γ . Representative images of HepG2 cells, as well as quantification of ORO isopropanol extracts of HepG2 and Huh7 cells, demonstrate that GDF10 reduced cellular lipid content in response to CGTZ treatment (Figure 4A,B; *, $p < 0.05$).

To follow up with our *in vivo* observations, we next examined the ability of GDF10 to modulate the nuclear abundance of C/EBP α as well as PPAR γ in Huh7 cells. Consistent with the livers of GDF10 $^{-/-}$ mice, immunoblot analysis of subcellular fractions in cultured hepatocytes revealed that GDF10 blocked the CGTZ-mediated nuclear localization of C/EBP α , and abundance of PPAR γ (Figure 4C). In line with subcellular fraction data, immunofluorescent staining of HepG2 and primary human hepatocytes also demonstrated that GDF10 blocked the

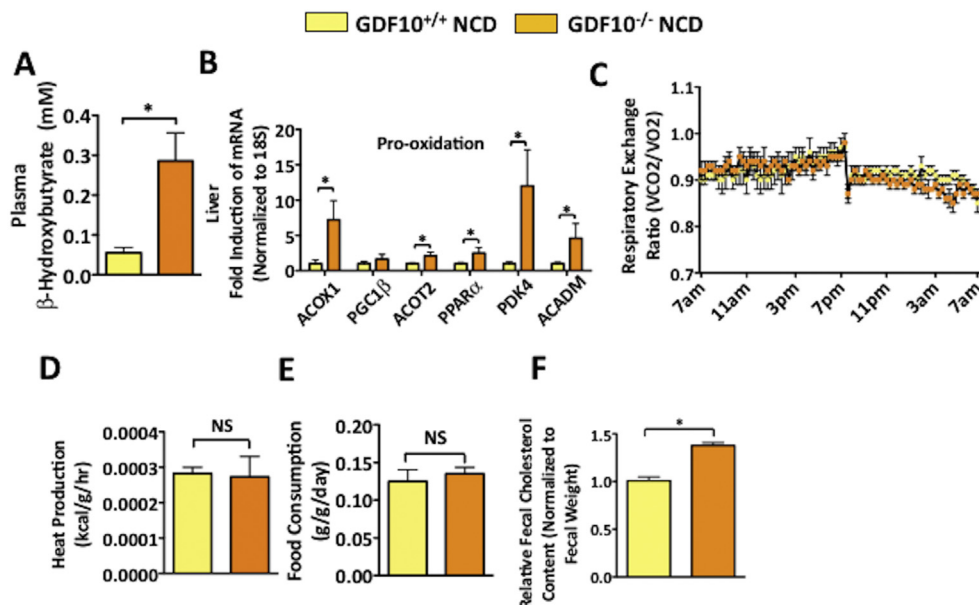


Figure 5: $GDF10^{-/-}$ mice exhibit compensatory changes in lipid homeostasis. (A) Plasma β -HB content (n = 5). (B) Real time PCR analysis of hepatic mRNA abundance of the indicated genes. (C) Respiratory exchange ratio (D) heat production and (E) food consumption in $GDF10^{+/+}$ and $GDF10^{-/-}$ mice fed NCD (n = 5). (F) Biliary cholesterol excretion in $GDF10^{+/+}$ and $GDF10^{-/-}$ mice fed NCD. All data are shown as the mean \pm S.D. *, $p < 0.05$ by unpaired two-tailed Student's t -test.

CGTZ-mediated nuclear localization of these transcription factors (Fig. S3A,S3B). Finally, the antagonistic effect of GDF10 on PPAR γ transcriptional activity was also confirmed in HepG2 cells using the transcription factor activity assay (Figure 4D; *, $p < 0.05$).

We next utilized this cultured hepatocyte model to determine the mechanism by which GDF10 affects PPAR γ expression and activity. Importantly, previous studies have demonstrated that (a) signaling of TGF β through TGF β receptor subtype-1 (TGF β R1) induces the phosphorylation of Smad3, which (b) leads to the suppression of PPAR γ expression and activity [35,36]. Furthermore, recent studies have also shown that (c) in a manner similar to TGF β , GDF10 induces the phosphorylation of Smad3 [35]. Similar to previous studies, we observed that exogenously-added rhGDF10 induced the phosphorylation of Smad3, but only in the absence of the TGF β R1 antagonist, IN1130. Also consistent with previous studies, rhGDF10 and/or IN1130 did not affect the phosphorylation of Smad1/5/9 (Figure 4E). Using the PPAR γ transcription factor assay, we next observed that rhGDF10 failed to antagonize CGTZ-mediated PPAR γ activity in cells transfected with small interfering (si)RNA targeted against Smad3 (siSmad3; Figure 4F; *, $p < 0.05$). This observation was also confirmed via immunofluorescent staining of PPAR γ and C/EBP α in Huh7 cells (Figure 4G). No marked change in cytotoxicity or cell morphology was observed in these cells (Figure 4H) and effective knockdown of Smad3 was confirmed via immunoblotting (Figure 4I). Finally, in line with these findings, we also observed that IN1130 attenuated the lipid-lowering effect of rhGDF10 in the presence of CGTZ (Fig. S4). Taken together, our results indicate that GDF10 acts to oppose PPAR γ -mediated lipid accumulation in cultured hepatocyte models via TGF β R1-induced Smad3 phosphorylation.

3.4. $GDF10^{-/-}$ mice exhibit compensatory changes in fatty acid oxidation

Other parameters known to contribute to fatty liver and/or obesity, such as changes in lipid oxidation, biliary cholesterol excretion, energy expenditure and food consumption were also examined in $GDF10^{-/-}$

mice. To examine the possibility of lipid accumulation occurring as a result of reduced fatty acid oxidation, the ketogenic marker β -HB, was measured in the plasma. Interestingly, the elevated levels of β -HB observed in NCD-fed $GDF10^{-/-}$ mice are indicative of increased global fatty acid oxidation (Figure 5A; *, $p < 0.05$), likely working as a compensatory mechanism to oppose further lipid accumulation. Consistent with this result, increased hepatic mRNA transcript levels of a number of known drivers of fatty acid oxidation, including acyl-coenzyme A oxidase (ACOX1), peroxisome proliferator-activated receptor gamma coactivator 1- β (PGC1 β), acyl-coenzyme A thioesterase 2 (ACOT2), peroxisome proliferator-activated receptor α (PPAR α), pyruvate dehydrogenase lipoamide kinase isozyme 4 (PDK4) and acyl-coenzyme A dehydrogenase, C-4 to C-12 straight chain (ACADM) were also observed in the livers of NCD-fed $GDF10^{-/-}$ mice (Figure 5B; *, $p < 0.05$). However, no difference in respiratory exchange ratio and heat production was detected between $GDF10^{+/+}$ and $GDF10^{-/-}$ mice (Figure 5C,D. *, $p < 0.05$). In addition, no difference in food consumption was observed between $GDF10^{+/+}$ and $GDF10^{-/-}$ mice (Figure 5E. *, $p < 0.05$). Increased fecal cholesterol content was also observed in the $GDF10^{-/-}$ mice, suggesting heightened biliary cholesterol excretion (Figure 5F; *, $p < 0.05$). Collectively, these data suggest that despite increased liver fat content observed in $GDF10^{-/-}$ mice, a variety of compensatory mechanisms act in tandem to attenuate further lipid accumulation.

3.5. $GDF10^{-/-}$ mice exhibit increased UPR activation, fibrosis and liver injury

ER stress is a well-established early initiator of hepatic steatosis and is known to contribute to the progression of liver disease [7,37,38]. Therefore, our next aim was to assess the expression of ER stress markers in the livers of NCD- and HFD-fed $GDF10^{-/-}$ mice. Consistent with the observed increase in hepatic triglyceride levels, histological analysis revealed increased expression of ER stress markers, glucose regulated protein of 78 and 94 kDa (GRP78, GRP94) as well as phosphorylated (p)PERK in response to a HFD in the livers $GDF10^{-/-}$

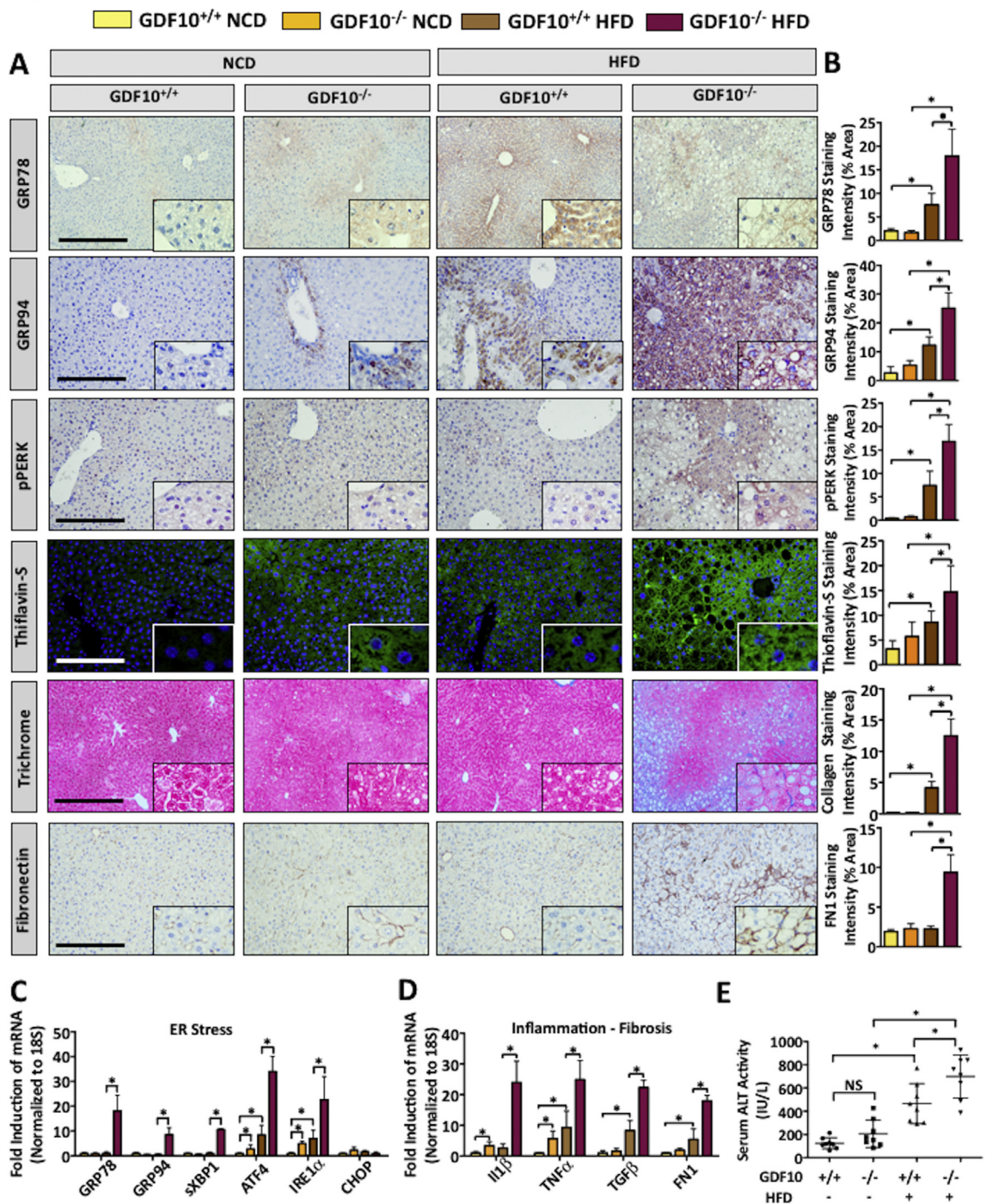


Figure 6: Livers from GDF10^{-/-} mice exhibit increased UPR activation, fibrosis, and inflammation. (A) IHC staining of GRP78, GRP94, pPERK and fibronectin, as well as Masson's Trichrome and Thioflavin-S in the livers of NCD- and HFD-fed mice. (B) Quantification of indicated histological staining (n = 5). Real time PCR analysis of hepatic mRNA abundance of the indicated genes involved in (C) ER stress, (D) inflammation, and fibrosis. (E) Analysis of serum ALT activity, a marker of liver injury (n = 8). Scale bars, 100 μ m. All data are shown as the mean \pm S.D. *, $p < 0.05$ by one-way ANOVA.

mice (Figure 6A,B; *, $p < 0.05$). Thioflavin-S staining of misfolded protein amyloid, known to occur as a result of prolonged ER stress [9] was also increased in HFD-fed GDF10^{-/-} mice compared to controls. Further assessment of the livers via IHC staining of fibronectin and Masson's Trichrome also revealed increased fibrosis in HFD-fed GDF10^{-/-} mice (Figure 6A,B; *, $p < 0.05$, n = 5). Increased

fibrosis in the livers of HFD-fed GDF10^{-/-} mice was also independently confirmed via Picosirius red (PSR) staining of fibrotic collagen deposition (Fig. S5A). Although a marked increase in ER stress and fibrosis markers was observed in the livers of HFD-fed GDF10^{-/-} mice, no substantial difference was observed in the NCD-fed cohort. mRNA transcript abundance of ER stress, fibrotic, inflammatory, and

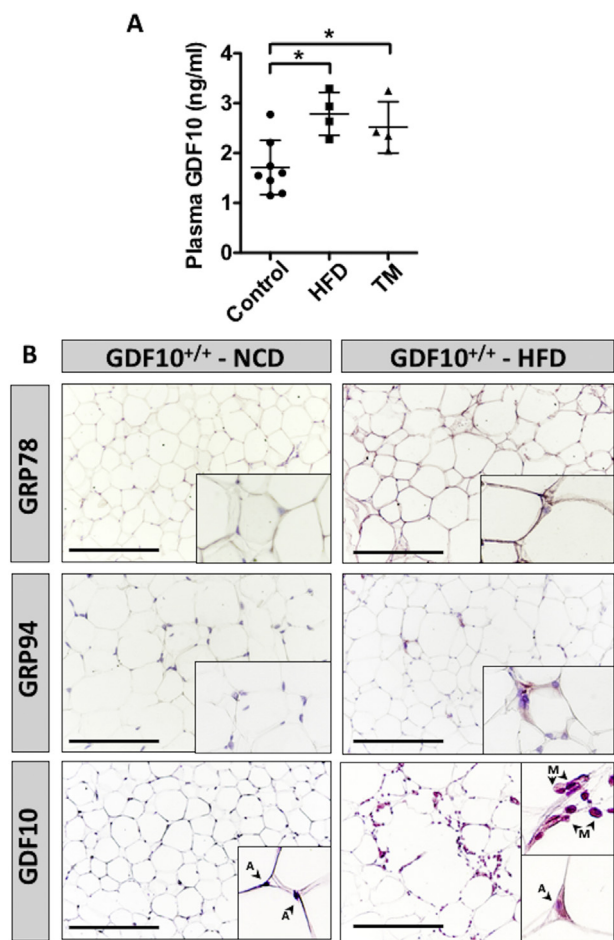


Figure 7: ER stress increases GDF10 abundance in GAT and in circulation. (A) Plasma content of circulating GDF10 in mice fed NCD or HFD for 12 weeks ($n = 5$), and mice treated with a bolus injection of TM (250 $\mu\text{g}/\text{kg} - 24 \text{ h}$; $n = 5$). (B) IHC staining of GRP78, GRP94 and GDF10 in the GAT of mice fed NCD or HFD. Scale bars, 100 μm . A and M indicate adipocytes and macrophages, respectively. All data are shown as the mean \pm S.D. *, $p < 0.05$ by one-way ANOVA.

apoptotic markers was also examined by real time PCR and yielded consistent findings with histological analysis (Figure 6C, D and Fig. S5B; *, $p < 0.05$, $n = 5$).

Hepatic insulin resistance represents another hallmark feature of liver disease. Thus, markers of hepatic gluconeogenesis were assessed via real time PCR. Interestingly, the gluconeogenic markers induced in the livers GDF10^{-/-} mice, including signal transducer and activator of transcription 3 (STAT3), CREB-regulated transcription cofactor 2 (CRT2), forkhead box protein O1 (FOXO1) and phosphoenolpyruvate carboxykinase 1 (PCK1) are also known to be upregulated by conditions of ER stress (Fig. S5C; *, $p < 0.05$) [39]. Finally, the enzymatic activity of circulating ALT was increased in the HFD-fed GDF10^{-/-} mice compared to NCD-fed controls, which is indicative of liver injury (Figure 6E; *, $p < 0.05$). Collectively, these data provide compelling evidence of heightened ER stress in the livers GDF10^{-/-} mice and highlight the ability of GDF10 to attenuate diet-induced liver injury.

3.6. ER stress increases circulating and adipose GDF10 levels

Given the role of GDF10 in the regulation of hepatic triglyceride levels and injury, our final aim was to assess the effect of diet-induced stress on GDF10 expression in GDF10^{+/+} mice. Similar to findings

demonstrating a positive correlation between circulating GDF15 levels and hepatic ER stress [24], we also observed increased plasma GDF10 levels in HFD-fed GDF10^{+/+} and in wild-type mice injected with the ER stress-inducing agent, TM (Figure 7A; *, $p < 0.05$, $n = 7$). Because GDF10 is primarily expressed in adipose tissue, we also examined whether TM affects GDF10 expression in 3T3-L1 adipocytes at day 10 of differentiation (Fig. S6; *, $p < 0.05$, $n = 5$) and in GAT from HFD-fed mice (Figure 7B; $n = 7$). Similar to secreted levels, an increase in GDF10 expression was observed in response to TM in 3T3-L1 adipocytes and in the GAT from HFD-fed GDF10^{+/+} mice. We also report the surprising finding that GAT-resident macrophages in HFD-fed mice express abundant levels of GDF10 (Figure 7B); an observation that was not present in GAT from NCD-fed mice. Collectively, these data suggest that during conditions of diet-induced stress, adipose tissue promotes the expression of GDF10 to attenuate further triglyceride accumulation in the liver as a response to injury.

4. DISCUSSION

A growing body of evidence suggests that GDF10, in addition to being a key modulator of osteogenesis, also plays a critical role in adipose lipid metabolism [20,21]. To the best of our knowledge, however, the functional importance of GDF10 in liver lipid metabolism has not yet been evaluated. Here, we demonstrate that GDF10^{-/-} mice exhibit increased adiposity, as well as increased body weight and hepatic triglyceride and cholesterol levels; an early feature in the development of diet-induced liver disease [3]. We also observed that severe lipid accumulation in the livers of HFD-fed GDF10^{-/-} mice was associated with a substantial induction of a variety of ER stress markers and concomitant liver injury. Additional hallmark characteristics of liver disease, such as apoptosis, inflammation, fibrosis and changes in gluconeogenic gene expression, were also observed in the livers of HFD-fed GDF10^{-/-} mice.

To explain these findings, we examined a number of metabolic parameters and expression of genes known to alter lipid metabolism. Despite elevated body weight and adiposity, an increase in global fatty acid oxidation was observed in GDF10^{-/-} mice. Given that this finding is in mechanistic contrast to the obese phenotype in the mice, these findings suggest that heightened fatty acid oxidation likely occurred as a compensatory response to attenuate further fat accumulation. In line with these data, an increase in biliary cholesterol excretion was also identified. To this end, we observed an increase in the expression of key modulators of adipogenesis and well-known drivers of NAFLD, such as PPAR γ and C/EBP α , in the livers of GDF10^{-/-} mice. Upon further analysis using cultured hepatocytes, exogenously added rhGDF10 reduced the abundance and transcriptional activity of PPAR γ , and also blocked PPAR γ agonist-driven lipid accumulation. Lastly, we have also demonstrated that GDF10 inhibits PPAR γ transcriptional activity via the conventional TGF β R1-Smad3 signaling cascade. Collectively, these data suggest that GDF10 is a potent antagonist of PPAR γ and can protect from diet-induced hepatic steatosis.

Several groups have recently demonstrated the involvement of multiple TGF β superfamily members in the pathogenesis of obesity-related diseases such as type 2 diabetes and NAFLD [40–42]. In clinical studies, GDF15 expression correlates with a variety of metabolic disorders, including obesity, insulin resistance and the risk of cardiovascular events [43]. GDF15^{-/-} mice also exhibit increased body weight and peripheral lipid accumulation following a metabolic challenge, whereas overexpression of this protein led to reduced body weight and improved metabolic parameters [44,45]. Similar to GDF15^{-/-} mice, GDF10^{-/-} mice have increased body weight and

adiposity, a phenotype that unlike $GDF15^{-/-}$ mice, does not require a metabolic stimulus such as a HFD. Our findings are also consistent with studies in which overexpression of GDF10 in mice led to a reduction in adiposity and improved metabolic outcomes [21].

Activation of the TGF β signaling cascade has been shown to differentially modulate the expression of lipogenic markers, based on tissue/cell-specific expression, and unique molecular interactions with a variety of inhibitory molecules and receptor–ligand complexes. TGF β signaling has been shown to induce lipogenesis, inflammation and cell death via Smad2/3 [42], while also blocking PPAR γ expression, activity and lipogenesis in a manner dependent on β -catenin [46]. Overexpression of Smad3 and its partner Smad4 has been shown to reduce PPAR γ promoter activity in aortic smooth muscle cells [47]. Furthermore, TGF β suppresses PPAR γ expression and activity via Smad3/4 binding to the inhibitory element in the PPAR promoter region in lung fibroblasts [36]. Given that GDF10 can induce the phosphorylation and activation of Smad3, but also block the transcriptional activation of PPAR γ , our data suggest that in a manner similar to TGF β , GDF10 reduces PPAR γ activity in a Smad3-dependent manner.

PPAR γ activation is necessary and sufficient to induce adipocyte differentiation. Studies have demonstrated that (a) selective ablation of PPAR γ , using a tamoxifen-dependent recombination system in mice, led to the death of adipocytes only a few days following treatment [48], and (b) AAV-mediated hepatic overexpression of PPAR γ_2 in mice promoted an adipose-like phenotype in hepatocytes by inducing the expression of pro-adipogenic mediators, such as adiponectin, and aP2, which resulted in severe steatosis [49]. Moreover, previous studies have also demonstrated that hepatic PPAR γ is robustly induced in the livers of patients, as well as in pre-clinical models of NAFLD [13,49]. Conversely, PPAR γ deletion in mouse hepatocytes has been shown to attenuate intracellular lipid accumulation [50]. Consistent with our studies, it is also well-established that exposure of mice to a HFD promotes the expression of hepatic PPAR γ and a variety of its downstream targets [51]. In addition to PPAR γ , we also observed increased expression and nuclear localization of C/EBP α in the livers of $GDF10^{-/-}$ mice compared to the $GDF10^{+/+}$ controls. C/EBP α is also known to play a crucial role in adipocyte differentiation, and similar to PPAR γ , its expression is both necessary and sufficient for adipogenesis [52]. Studies also demonstrate that C/EBP α can directly regulate PPAR γ promoter activity [53] and has been described as a critical and obligate regulator of PPAR γ expression [54]. Furthermore, PPAR γ and C/EBP α mutually induce each other's expression in order to promote adipogenesis [53,55,56]. Given the cross-talk that occurs between these two master regulators of adipogenesis, it remains unclear which of the two, or whether both are directly affected by GDF10.

In summary, we demonstrate that GDF10 is an essential modulator of hepatic lipid homeostasis and is crucial for the maintenance of hepatic lipid turnover. GDF10 knockout leads to hepatic steatosis in NCD-fed mice, as well as severe steatosis, inflammation, fibrosis, and ER stress in response to a HFD. Given that most diet-induced models of liver disease fail to recapitulate fibrosis, a key marker of NASH, in this report we also describe a new genetic model for the study of liver disease. Furthermore, conditions that cause hepatic and/or adipocyte lipid accumulation also induced a compensatory increase in circulating GDF10 levels in $GDF10$ -expressing control mice. Additional tissue-specific knockdown studies, however, are required to confirm the origin of circulating GDF10 in the context of diet-induced NAFLD. Future studies examining the correlation between polymorphisms in the $GDF10$ gene and the prevalence of obesity and/or NAFLD may also

yield interesting findings. Overall, we identify circulating GDF10 as a novel regulator of liver lipid metabolism and demonstrate that in a manner similar to GDF15, this adipokine could be utilized for the management of metabolic disorders.

FINANCIAL SUPPORT

This work was supported in part by research grants to Richard C. Austin from the Heart and Stroke Foundation of Canada (G-13-0003064 and G-15-0009389) and the Canadian Institutes of Health Research (74477, 111239). Financial support from the Research Institute of St. Joe's Hamilton is acknowledged. Richard C. Austin is a Career Investigator of the Heart and Stroke Foundation of Ontario and holds the Amgen Canada Research Chair in the Division of Nephrology at St. Joseph's Healthcare Hamilton and McMaster University. Kenneth N. Maclean gratefully acknowledges financial support from the William R. Hummel Homocystinuria Research Fund and holds the Eht-Hummel-Kaufmann Family Endowed Chair in Inherited Metabolic Disease.

AUTHOR CONTRIBUTIONS

KP, PL, and RCA conceived the studies and wrote the manuscript. KP, PL, JHB, SVP, EAD, MEM, and AMB performed all of the *in vitro* and *in vivo* studies. The manuscript was revised by KNM and JCK.

CONFLICT OF INTEREST

The authors declare that they have no conflicts of interest with the contents of this article.

APPENDIX A. SUPPLEMENTARY DATA

Supplementary data to this article can be found online at <https://doi.org/10.1016/j.molmet.2019.06.021>.

REFERENCES

- [1] Gonzalez-Muniesa, P., Martinez-Gonzalez, M.A., Hu, F.B., Despres, J.P., Matsuzawa, Y., Loos, R.J.F., et al., 2017. Obesity. *Nature Reviews Disease Primers* 3:17034.
- [2] Perry, R.J., Samuel, V.T., Petersen, K.F., Shulman, G.I., 2014. The role of hepatic lipids in hepatic insulin resistance and type 2 diabetes. *Nature* 510: 84–91.
- [3] Brunt, E.M., Wong, V.W., Nobili, V., Day, C.P., Sookoian, S., Maher, J.J., et al., 2015. Nonalcoholic fatty liver disease. *Nature reviews Disease primers* 1: 15080.
- [4] Angulo, P., 2002. Nonalcoholic fatty liver disease. *New England Journal of Medicine* 346:1221–1231.
- [5] Kim, J.Y., Garcia-Carbonell, R., Yamachika, S., Zhao, P., Dhar, D., Loomba, R., et al., 2018. ER stress drives lipogenesis and steatohepatitis via caspase-2 activation of S1P. *Cell* 75:133–145 e115.
- [6] Ashraf, N.U., Sheikh, T.A., 2015. Endoplasmic reticulum stress and oxidative stress in the pathogenesis of non-alcoholic fatty liver disease. *Free Radical Research* 49:1405–1418.
- [7] Puri, P., Mirshahi, F., Cheung, O., Natarajan, R., Maher, J.W., Kellum, J.M., et al., 2008. Activation and dysregulation of the unfolded protein response in nonalcoholic fatty liver disease. *Gastroenterology* 134:568–576.
- [8] Zeng, L., Lu, M., Mori, K., Luo, S., Lee, A.S., Zhu, Y., et al., 2004. ATF6 modulates SREBP2-mediated lipogenesis. *The EMBO Journal* 23:950–958.

- [9] Zhou, H., Liu, R., 2014. ER stress and hepatic lipid metabolism. *Frontiers in Genetics* 5:112.
- [10] Bobrovnikova-Marjon, E., Hatzivassiliou, G., Grigoriadou, C., Romero, M., Cavener, D.R., Thompson, C.B., et al., 2008. PERK-dependent regulation of lipogenesis during mouse mammary gland development and adipocyte differentiation. *Proceedings of the National Academy of Sciences of the United States of America* 105:16314–16319.
- [11] Matsusue, K., Kusakabe, T., Noguchi, T., Takiguchi, S., Suzuki, T., Yamano, S., et al., 2008. Hepatic steatosis in leptin-deficient mice is promoted by the PPAR gamma target gene *Fsp27*. *Cell Metabolism* 7:302–311.
- [12] Lee, Y.J., Ko, E.H., Kim, J.E., Kim, E., Lee, H., Choi, H., et al., 2012. Nuclear receptor PPAR γ -regulated monoacylglycerol O-acyltransferase 1 (MGAT1) expression is responsible for the lipid accumulation in diet-induced hepatic steatosis. *Proceedings of the National Academy of Sciences of the United States of America* 109:13656–13661.
- [13] Pettinelli, P., Videla, L.A., 2011. Up-regulation of PPAR- γ mRNA expression in the liver of obese patients: an additional reinforcing lipogenic mechanism to SREBP-1c induction. *Journal of Clinical Endocrinology & Metabolism* 96:1424–1430.
- [14] Zhang, X.Q., Xu, C.F., Yu, C.H., Chen, W.X., Li, Y.M., 2014. Role of endoplasmic reticulum stress in the pathogenesis of nonalcoholic fatty liver disease. *World Journal of Gastroenterology* 20:1768–1776.
- [15] Matsumoto, Y., Otsuka, F., Hino, J., Miyoshi, T., Takano, M., Miyazato, M., et al., 2012. Bone morphogenetic protein-3b (BMP-3b) inhibits osteoblast differentiation via Smad2/3 pathway by counteracting Smad1/5/8 signaling. *Molecular and Cellular Endocrinology* 350:78–86.
- [16] Zhao, R., Lawler, A.M., Lee, S.J., 1999. Characterization of GDF-10 expression patterns and null mice. *Developmental Biology* 212:68–79.
- [17] Tseng, Y.H., Kokkotou, E., Schulz, T.J., Huang, T.L., Winnay, J.N., Taniguchi, C.M., et al., 2008. New role of bone morphogenetic protein 7 in brown adipogenesis and energy expenditure. *Nature* 454:1000–1004.
- [18] Schulz, T.J., Tseng, Y.H., 2009. Emerging role of bone morphogenetic proteins in adipogenesis and energy metabolism. *Cytokine & Growth Factor Reviews* 20:523–553.
- [19] Zamani, N., Brown, C.W., 2011. Emerging roles for the transforming growth factor- β superfamily in regulating adiposity and energy expenditure. *Endocrine Reviews* 32:387–403.
- [20] Hino, J., Miyazawa, T., Miyazato, M., Kangawa, K., 2012. Bone morphogenetic protein-3b (BMP-3b) is expressed in adipocytes and inhibits adipogenesis as a unique complex. *International Journal of Obesity* 36:725–734.
- [21] Hino, J., Nakatani, M., Arai, Y., Tsuchida, K., Shirai, M., Miyazato, M., et al., 2017. Overexpression of bone morphogenetic protein-3b (BMP-3b) in adipose tissues protects against high-fat diet-induced obesity. *International Journal of Obesity* 41:483–488.
- [22] Chrysovergis, K., Wang, X., Kosak, J., Lee, S.H., Kim, J.S., Foley, J.F., et al., 2014. NAG-1/GDF-15 prevents obesity by increasing thermogenesis, lipolysis and oxidative metabolism. *International Journal of Obesity* 38:1555–1564.
- [23] Li, D., Zhang, H., Zhong, Y., 2018. Hepatic GDF15 is regulated by CHOP of the unfolded protein response and alleviates NAFLD progression in obese mice. *Biochemical and Biophysical Research Communications* 498:388–394.
- [24] Tsai, V.W.W., Husaini, Y., Sainsbury, A., Brown, D.A., Breit, S.N., 2018. The MIC-1/GDF15-GFRAL pathway in energy homeostasis: implications for obesity, cachexia, and other associated diseases. *Cell Metabolism* 28:353–368.
- [25] Polyzos, S.A., Kountouras, J., Mantzoros, C.S., 2016. Adipokines in nonalcoholic fatty liver disease. *Metabolism Clinical and Experimental* 65:1062–1079.
- [26] Lebeau, P., Platko, K., Al-Hashimi, A.A., Byun, J.H., Lhotak, S., Holzapfel, N., et al., 2018. Loss-of-function PCSK9 mutants evade the unfolded protein response sensor GRP78 and fail to induce endoplasmic reticulum stress when retained. *Journal of Biological Chemistry* 293:7329–7343.
- [27] Lebeau, P.F., Byun, J.H., Platko, K., MacDonald, M.E., Poon, S.V., Faiyaz, M., de novo PCSK9 expression in mice. *Journal of Biological Chemistry* 294:9037–9047.
- [28] Lee, J.S., Zheng, Z., Mendez, R., Ha, S.W., Xie, Y., Zhang, K., 2012. Pharmacologic ER stress induces non-alcoholic steatohepatitis in an animal model. *Toxicology Letters* 211:29–38.
- [29] Gross, B., Pawlak, M., Lefebvre, P., Staels, B., 2017. PPARs in obesity-induced T2DM, dyslipidaemia and NAFLD. *Nature Reviews Endocrinology* 13:36–49.
- [30] Bocos, C., Göttlicher, M., Gearing, K., Banner, C., Enmark, E., Teboul, M., et al., 1995. Fatty acid activation of peroxisome proliferator-activated receptor (PPAR). *The Journal of Steroid Biochemistry and Molecular Biology* 53:467–473.
- [31] Krey, G., Braissant, O., L'Horsset, F., Kalkhoven, E., Perroud, M., Parker, M.G., et al., 1997. Fatty acids, eicosanoids, and hypolipidemic agents identified as ligands of peroxisome proliferator-activated receptor by coactivator-dependent receptor ligand assay. *Molecular Endocrinology* 6:779–791.
- [32] Ahmad, I., Mui, E., Galbraith, L., Patel, R., Tan, E.H., Salji, M., et al., 2016. Sleeping beauty screen revealed ppar γ activation in metastatic prostate cancer. *Proceedings of the National Academy of Sciences* 29:8290–8295.
- [33] Jiang, Y., Thakran, S., Bheemreddy, R., Ye, E.A., He, H., Walker, R.J., et al., 2014. Pioglitazone normalizes insulin signaling in the diabetic rat retina through reduction in tumor necrosis factor α and suppressor of cytokine signaling 3. *Journal of Biological Chemistry* 289:26395–26405.
- [34] De Vos, P., Lefebvre, A.M., Miller, S.G., Guerre-Millo, M., Wong, K., Saladin, R., et al., 1996. Thiazolidinediones repress ob gene expression in rodents via activation of peroxisome proliferator-activated receptor gamma. *Journal of Clinical Investigation* 98:1004–1009.
- [35] Upadhyay, G., Yin, Y., Yuan, H., Derynch, R., Glazer, R.I., 2011. Stem cell antigen-1 enhances tumorigenicity by disruption of growth differentiation factor-10 (GDF10)-dependent TGF- β signaling. *Proceedings of the National Academy of Sciences of the United States of America* 108:7820–7825.
- [36] Lakshmi, S.P., Reddy, A.T., Reddy, R.C., 2017. Transforming growth factor β suppresses peroxisome proliferator-activated receptor γ expression via both SMAD binding and novel TGF- β inhibitory elements. *Biochemical Journal* 474:1531–1546.
- [37] Wang, D., Wei, Y., Pagliassotti, M.J., 2006. Saturated fatty acids promote endoplasmic reticulum stress and liver injury in rats with hepatic steatosis. *Endocrinology* 147:943–951.
- [38] Bashiri, A., Nesan, D., Tavallaee, G., Sue-Chu-Lam, I., Chien, K., Maguire, G.F., et al., 2016. Cellular cholesterol accumulation modulates high fat high sucrose (HFHS) diet-induced ER stress and hepatic inflammasome activation in the development of non-alcoholic steatohepatitis. *Biochimica et Biophysica Acta* 1861:594–605.
- [39] Kim, O.K., Jun, W., Lee, J., 2015. Mechanism of ER Stress and inflammation for hepatic insulin resistance in obesity. *Annals of Nutrition & Metabolism* 67:218–227.
- [40] Yadav, H., Quijano, C., Kamaraju, A.K., Gavrilova, O., Malek, R., Chen, W., et al., 2011. Protection from obesity and diabetes by blockade of TGF- β /Smad3 signaling. *Cell Metabolism* 14:67–79.
- [41] Margoni, A., Fotis, L., Papavassiliou, A.G., 2012. The transforming growth factor-beta/bone morphogenetic protein signalling pathway in adipogenesis. *The International Journal of Biochemistry & Cell Biology* 44:475–479.
- [42] Yang, L., Roh, Y.S., Song, J., Zhang, B., Liu, C., Loomba, R., et al., 2014. Transforming growth factor beta signaling in hepatocytes participates in steatohepatitis through regulation of cell death and lipid metabolism in mice. *Hepatology* 59:483–495.
- [43] Kempf, T., Guba-Quint, A., Torgerson, J., Magnone, M.C., Haefliger, C., Bobadilla, M., et al., 2012. Growth differentiation factor 15 predicts future insulin resistance and impaired glucose control in obese nondiabetic individuals: results from the XENDOS trial. *European Journal of Endocrinology* 167:671–678.
- [44] Macia, L., Tsai, V.W., Nguyen, A.D., Johnen, H., Kuffner, T., Shi, Y.C., et al., 2012. Macrophage inhibitory cytokine 1 (MIC-1/GDF15) decreases food intake,

- body weight and improves glucose tolerance in mice on normal & obesogenic diets. *PLoS One* 7:e34868.
- [45] Kim, J.M., Kosak, J.P., Kim, J.K., Kissling, G., Germolec, D.R., Zeldin, D.C., et al., 2013. NAG-1/GDF15 transgenic mouse has less white adipose tissue and a reduced inflammatory response. *Mediators of Inflammation* 2013:641851.
- [46] Qian, J., Niu, M., Zhai, X., Zhou, Q., Zhou, Y., 2012. Beta-catenin pathway is required for TGF- β 1 inhibition of PPAR γ expression in cultured hepatic stellate cells. *Pharmacological Research* 66:219–225.
- [47] Fu, M., Zhang, J., Lin, Y., Zhu, X., Zhao, L., Ahmad, M., et al., 2003. Early stimulation and late inhibition of peroxisome proliferator-activated receptor gamma (PPAR gamma) gene expression by transforming growth factor beta in human aortic smooth muscle cell: role of early growth-response factor-1 (Egr-1), activator protein 1 (AP1) and Smads. *Biochemical Journal* 370:1019–1025.
- [48] Imai, T., Takakuwa, R., Marchand, S., Dentz, E., Bornert, J.M., Messaddeq, N., et al., 2004. Peroxisome proliferator-activated receptor gamma is required in mature white and brown adipocytes for their survival in the mouse. *Proceedings of the National Academy of Sciences of the United States of America* 101:4543–4547.
- [49] Yu, S., Matsusue, K., Kashireddy, P., Cao, W.Q., Yeldandi, V., Yeldandi, A.V., et al., 2003. Adipocyte-specific gene expression and adipogenic steatosis in the mouse liver due to peroxisome proliferator-activated receptor γ 1 (PPAR γ 1) overexpression. *Journal of Biological Chemistry* 278:498–505.
- [50] Moran-Salvador, E., Lopez-Parr, M., Garcia-Alonso, V., Titos, E., Martinez-Clemente, M., Gonzalez-Periz, A., et al., 2011. Role of PPAR γ in obesity-induced hepatic steatosis as determined by hepatocyte- and macrophage-specific conditional knockouts. *Federation of American societies of Experimental Biology* 25:2538–2550.
- [51] Inoue, M., Ohtake, T., Motomura, W., Takahashi, N., Hosoki, Y., Miyoshi, S., et al., 2005. Increased expression of PPAR γ in high fat diet-induced liver steatosis in mice. *Biochemical and Biophysical Research Communications* 336:215–222.
- [52] Lane, M.D., Tang, Q.Q., Jiang, M.S., 1999. Role of the CCAAT enhancer binding proteins (C/EBPs) in adipocyte differentiation. *Biochemical and Biophysical Research Communications* 3:677–683.
- [53] Clarke, S.L., Robinson, C.E., Gimble, J.M., 1997. CAAT/enhancer binding proteins directly modulate transcription from the peroxisome proliferator-activated receptor γ 2 promoter. *Biochemical and Biophysical Research Communications* 1:99–103.
- [54] Madsen, M.S., Siersbaek, R., Boergesen, M., Nielsen, R., Mandrup, S., 2014. Peroxisome proliferator-activated receptor gamma and C/EBPalpha synergistically activate key metabolic adipocyte genes by assisted loading. *Molecular and Cellular Biology* 34:939–954.
- [55] Wu, Z., Rosen, E., Brun, R., Hauser, S., Adelmant, G., Troy, A., 1999. Cross regulation of C/EBP α and PPAR γ controls the transcriptional pathway of adipogenesis and insulin sensitivity. *Molecular Cell* 3:151–158.
- [56] Elberg, G., Gimble, J., Tsai, S., 2000. Modulation of the murine peroxisome proliferator-activated receptor γ 2 promoter activity by CCAAT/enhancer-binding proteins. *Journal of Biological Chemistry* 275:27815–27822.